GMR
The Original

PRODUCING HIGH-PURITY INULIN POWDER FROM CHICORY ROOTS

Gurumukh Singh[1], Apoorva Behari Lal[1], Ashish Khare[1], Amit Pratap Singh[1]

[1]R.B.S. Engineering Technical Campus, Bichpuri, Agra is affiliated with Dr. A.P.J. Abdul Kalam Technical University Lucknow, Email: gurumukhsingh1992@yahoo.com

ABSTRACT

The suitability of an inulin powder to be used in pharmaceutical applications is primarily based on its purity; however, inulin extracted from the conventional extraction trains is frequently contaminated with free sugars, proteins and pigments. A systematic process for the development and optimisation of an integrated process for the production of high-purity inulin from chicory (Cichorium intybus L.) roots based on hot-water extraction, membrane purification and spray drying is developed. The Box–Behnken design was implemented to optimise hot-water extraction and evaluated by three factors: namely, temperature, solid-to-liquid ratio and extraction time. The fitted quadratic model was significant ($p < 0.001$) with $R^2 = 0.972$ and a non-significant lack-of-fit ($p = 0.18$); the predicted optimum (80 °C, 1:15 g mL^{-1}, 60 min) gave an inulin recovery of 84.2 ± 1.5%, agreeing with the model prediction within 3%. The clarified extract was refined by microfiltration followed by nanofiltration with diafiltration, raising inulin purity from 71.3 ± 2.4% to 93.6 ± 1.3% of dry solids, although a measurable decline in permeate flux indicated membrane fouling. The nanofiltration concentrate (about 7 to 15 °Brix) was demineralised on a two-bed anion- and cation-exchange resin column to remove residual inorganic impurities and then concentrated by multiple-effect evaporation (about 15 to 35 °Brix) ahead of drying. Spray drying of the retentate, optimised for inlet air temperature and feed concentration, produced a low-moisture powder (4.6 ± 0.3%) at a yield of about 69%, with the main losses associated with wall deposition. The results indicate that an integrated, purification-focused workflow can deliver high-purity inulin from an inexpensive feedstock, and they provide a basis for future scale-up and pharmacopoeial qualification studies.

KEYWORDS: inulin; chicory roots; membrane purification; nanofiltration; ion-exchange demineralisation; response surface methodology; process optimisation; high-purity fructan; spray drying; process intensification.

1. INTRODUCTION

Inulin is a plant storage carbohydrate of the fructan family. Its chains are built from fructose units linked mainly by β-(2→1) bonds and usually capped by a terminal glucose. The degree of polymerisation varies widely, from a few units to more than sixty, and this spread in chain length controls properties such as solubility, viscosity, and the ability to form particle gels [1]. Because human digestive enzymes cannot cleave the β-(2→1) bond, inulin reaches the colon largely intact and is fermented there by beneficial bacteria. This physical and physiological lack of digestibility has made inulin a frequent fibre, fat replacer, and with its biochemical inertness, a prebiotic for food and related products [2].

The use of inulin in nutrition is no longer the only area in which it is used. Low toxicity and biodegradability characteristics of inulin-type fructans are useful in the studies of excipients and carriers for delivery systems [3]. It is also glass-forming, so it is protective when drying or storing sensitive ingredients. For these applications, however, a much purer raw material is required than what is used in normal food applications: a powder meant for pharmaceutical applications should not have too much reducing sugar, protein and pigment and must behave consistently in different batches.

Today, the roots of Chicory (Cichorium intybus L.) are still the principal industrial source of inulin. The main carbohydrate stored in the roots is inulin, which can represent more than fifteen to twenty per cent of the fresh weight, and chicory has a fairly wide range of tolerance for temperate growing conditions. Extraction from chicory has thus been extensively investigated, considering its impact on recovery % and quality according to the different temperature, time, solvent ratio and particle size [4]. Some studies also link downstream to the extraction and get purified inulin and part of the extraction as fructooligosaccharides [5]. Recent research has included a comparison to the more environmentally friendly alternative and has found that the method of extraction has an effect on the yield, distribution of molecular weight and functional quality [6].

Other kinds of feedstocks have been investigated in addition to chicory. A combined ultrasound- and ultrafiltration method has been used for agave, chicory and Jerusalem artichoke [7] and a combined ultrasound-assisted and extraction method applied to the burdock root [8]; Advanced inulin powders have been obtained by a combined microwave and ultimate filtration [9]. Jerusalem artichoke has received special attention in both the extraction of its components in different conditions [10] and in purification by using resin [11], as well as ohmic heating [12] and ohmic-ultrasonic extraction and drying [13]. In a recent process-development study, the hot water extraction, purification and drying for this source are even combined into one train [14]. Inulin-type fructans have also been extracted from dandelion root [15] and Agave sisalana [16] as well as from some inulin-containing common plants [17] and Stevia processing waste [18].

This portfolio includes some very good comparisons, but also primarily focuses on individual feedstocks and individual steps.

The quality of the product is affected by the route adopted for extraction. For instance, in the extraction process of chicori with acid, part of the polymer is broken down to produce fructose-rich extracts, which are beneficial for the sweetener production, but not where the high molecular weight polymer, inulin, is desired [19]. An attempt has been made to limit such damage by trying pulsed electric fields, which have helped in the extraction of chicory at pilot scale [20], have been used to extract juice from chicory [21] and have been tried on agave [22]. However, if shorter chains are desired, inulin can be enzymatically changed to fructooligosaccharides [23]. The general message of a recent review on Jerusalem artichoke inulin points to the expectations that choices of extraction and purification of inulin propagate throughout the value chain [24].

The drying step is just as important since it defines the properties of the powder, which are important for handling processes: moisture, flowability and reconstitution behaviour. Inulin has been physically well characterised and studied for its effect as a drying carrier to preserve antioxidants [25, 26]. The spray drying optimisation of chicory inulin has also been optimised [27], and inulin can even be used in the encapsulation of sensitive actives such as essential oils [28]. Inulin is a sugar-rich feed and is found to possess the stickiness and wall-deposition problems associated with it [29]. It is simultaneously a beneficial protection system in the treatment of probiotic bacteria during spray drying [30] and in single- and multi-layer mixture encapsulation, such as for plant-pigment extracts [34] and for bifidobacteria [33].

Despite all this literature, most studies attempt to optimise one unit operation alone, and the few integrated reports consider (in far less detail) downstream purity as the parameter to be optimised for the optimum of the upstream one. The present study does just that. The extraction optimum in this case is chosen to trade off for retention of the high molecular weight fraction that the nanofiltration membrane is supposed to retain, resulting in a co-design of the 3 stages and not just connecting them. Another, more specific feature of the workflow is that the nanofiltration permeate is not considered waste but a recoverable stream of fructooligosaccharides; also, the practical penalties for integration (membrane fouling, diafiltration water consumption and excretion losses due to drying) are not neglected but quantified.

The objectives are

(i) optimise the extraction of hot water at horizontal level, solid-to-liquid ratio and extraction period by Box-Behnken design; (iii) to upgrade the extract using a microfiltration/nanofiltration and anion–cation ion-exchange process, and (iii) to maximise the purified retentate spray drying efficiency. Qualification and formulation testing for the pharmacopoeia are not included in the scope, since these additions will occur in future works.

2. MATERIALS AND METHODS

2.1. Raw Material and Reagents

Fresh chicory (Cichorium intybus L.) roots were obtained from a single agricultural lot to limit compositional variability. Roots were washed, peeled, and sliced into chips of 3–5 mm thickness using a manual slicer; damaged or discoloured tissue was discarded. Chips were processed within 24 h or held at 4 °C for no longer than 48 h. The moisture content of the fresh roots was 77.2 ± 0.6% (wet basis), and the initial inulin content was 18.3 ± 0.7% of fresh weight, determined as described in Section 2.7. All reagents (chromatography-grade standards of inulin, fructose, glucose, and sucrose; inulinase enzyme; and analytical-grade salts and solvents) were of recognised analytical quality, and deionised water (conductivity < 2 μS cm^{-1}) was used throughout.

Prior to extraction, the roots were passed over a vibro screen (10 mesh) to remove adhering dust and fines, and then size-reduced in a hammer mill to a particle size of 3–5 mm to provide a uniform feed and improve mass transfer during extraction.

2.2. Hot-Water Extraction

Inulin was recovered by hot-water extraction in a 2 L jacketed glass vessel connected to a thermostatic circulating bath, with stirring at 150 rpm by an overhead paddle to keep contact uniform without excessive shear. Chips were combined with preheated deionised water at the prescribed solid-to-liquid ratio, and the temperature was held within ±1 °C of the set point. After the set time, the slurry was screened through a 250 μm stainless mesh to remove spent solids, and the extract was cooled rapidly in an ice bath to limit further hydrolysis. Temperature, solid-to-liquid ratio, and time were the three variables optimised, since they jointly govern the balance between inulin diffusion into the solvent and the co-extraction of impurities or partial thermal hydrolysis of the polymer. At this point the clarified liquor was sampled for in-process control, which typically gave 7–8 °Brix, an inulin content of about 80% of dissolved solids, and a pH of 6.5 ± 0.2. The coarse spent solids were separated by drum filtration over the 250 μm stainless mesh, after which the liquor was passed through a 25 μm press filter to remove residual fine particulates ahead of purification.

2.3. Experimental Design and Statistical Analysis

Extraction was optimised with a three-factor Box-Behnken design. The factors were extraction temperature (X_1), solid-to-liquid ratio (X_2), and extraction time (X_3), each studied at three coded levels (−1, 0, +1) as listed in Table 1. The design comprised 17 runs, including five replicated centre points used to estimate pure error; the full run matrix and the measured recovery for each run are given in Table 2. Inulin recovery (Y, %) — the mass of inulin transferred into the extract relative to that originally present in the root — was the response. A second-order polynomial of the form $Y = \beta_0 + \Sigma\beta_i X_i + \Sigma\beta_{ii} X_i^2 + \Sigma\beta_{ij} X_i X_j$ was fitted by least squares. Model significance, individual term significance, and lack-of-fit were assessed by analysis of variance at $\alpha = 0.05$, and model adequacy was judged from the coefficient of determination (R^2), adjusted R^2, and residual plots. Design generation and regression were carried out in Design-Expert (Stat-Ease). The predicted optimum was verified in triplicate, and agreement between predicted and observed recovery was used to confirm model validity. All other measurements were performed in triplicate and are reported as mean ± standard deviation.

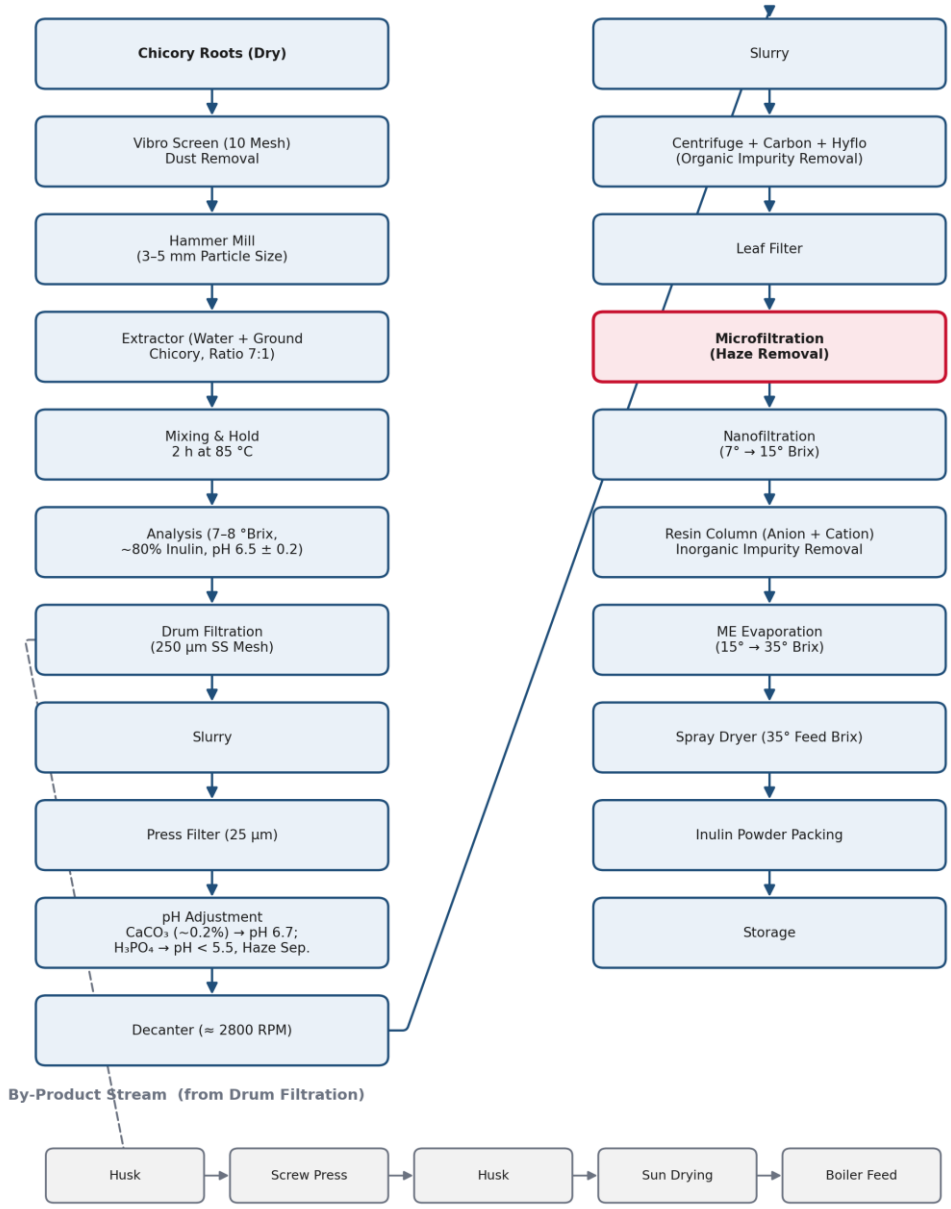

Figure 1. Process flow diagram for the production of purified inulin powder from chicory roots, from root pre-treatment through extraction, clarification, microfiltration, nanofiltration, ion-exchange demineralisation on anion and cation resin columns, multiple-effect evaporation, and spray drying to packing and storage. The spent solids are recovered as a by-product stream (husk → screw press → sun drying → boiler feed).

2.4. Membrane Filtration and Purification

The extract obtained at the optimum condition was purified in two membrane stages on a bench-scale cross-flow rig. Microfiltration used a 0.2 µm polyethersulfone membrane (effective area 0.1 m²) operated at a transmembrane pressure of 1.0 bar to remove fine particles and colloidal haze. The clarified permeate was then nanofiltered through a thin-film composite polyamide nanofiltration membrane of approximately 300 Da molecular-weight cut-off (effective area 0.1 m²) at a transmembrane pressure of 20 bar and a cross-flow velocity of about 1.5 m s^{-1}, with the feed kept at 25–30 °C. Because the nanofiltration stage retains water as well as the fructan fraction, it acted at the same time as a purification and a concentration step, raising the stream from about 7 °Brix to about 15 °Brix. High-molecular-weight inulin was retained while free sugars, short oligosaccharides, low-molecular-weight proteins, and coloured phenolics passed into the permeate. The retentate was then diafiltered with two diavolumes of deionised water to further lower residual low-molecular-weight solutes. Permeate flux was recorded over time to monitor fouling, and inulin purity was measured before and after each stage.

Ahead of the membrane stages, the press-filtered liquor was clarified by a lime/acid sequence. Calcium carbonate (≈0.2% w/v) was added to hold the pH near 6.7 and precipitate proteins and polyphenols, and phosphoric acid was then used to bring the pH below 5.5 to promote flocculation and separation of impurities. The bulk precipitate was removed in a decanter centrifuge (≈2800 rpm), and the liquor was further polished by centrifugation in the presence of activated carbon and Hyflo filter aid for organic-impurity and colour removal, followed by a leaf filter.

After microfiltration and nanofiltration with diafiltration, the purified and partially concentrated stream (about 15 °Brix) was carried forward to ion-exchange demineralisation and evaporative concentration, which are described in Section 2.5.

2.5. Ion-Exchange Demineralisation and Evaporative Concentration

The inorganic impurities that pass through the membrane stages — principally calcium, magnesium, sodium and potassium together with sulphate, chloride and phosphate carried over from the lime/acid clarification — were removed by ion exchange. The nanofiltration concentrate was demineralised on a two-bed resin column arranged in series, comprising a strongly acidic cation-exchange resin in the hydrogen form followed by a weakly basic anion-exchange resin in the free-base form. The cation bed exchanges the metal cations for hydrogen ions, and the anion bed then retains the mineral acids so generated, so that the combined effect of the two beds is the removal of dissolved salts together with a further reduction in residual organic acids and colour bodies. The beds (bed-volume ratio approximately 1:1) were operated at ambient temperature in downflow mode at a linear flow rate of about two bed volumes per hour, and the treated liquor was collected until the outlet conductivity rose above the set limit, at which point the columns were taken off line. Regeneration between cycles used dilute hydrochloric acid for the cation resin and dilute sodium hydroxide for the anion resin, each followed by rinsing with deionised water until the effluent was neutral. Conductivity and pH at the column outlet were recorded throughout as the in-process control for this stage.

The demineralised liquor was then concentrated by multiple-effect (ME) evaporation from about 15 °Brix to about 35 °Brix. Evaporation was carried out under vacuum so that the boiling temperature, and hence the thermal exposure of the fructan chains, was kept low, and it was placed ahead of the dryer to reduce the water load on the spray-drying stage. For the drying trials described in Section 2.6, the concentrate was adjusted with deionised water to the feed total-solids levels required by the experimental design.

2.6. Spray Drying

The purified retentate was dried in a laboratory spray dryer (Büchi B-290 type) fitted with a 0.7 mm two-fluid nozzle in co-current configuration. Two variables were studied: inlet air temperature (130, 150, and 170 °C) and feed total solids (8, 12, and 16% w/w). Feed flow rate (≈9 mL min^{-1}), aspirator rate (≈35 m^3 h^{-1}), and atomising air pressure (≈5 bar) were held constant so that the effects of the two principal variables could be isolated. Outlet air temperature was recorded for each run. Powder was collected from the cyclone, weighed to determine process yield, and stored in sealed amber containers over desiccant pending analysis. Wall deposition was noted qualitatively after each run as an indicator of stickiness-related losses.

2.7. Analytical and Characterisation Methods

Inulin content was quantified by the standard enzymatic-spectrophotometric fructan method: total fructose and glucose were measured before and after complete enzymatic hydrolysis with inulinase, and inulin was calculated from the increase in reducing sugars after correction for free sugars present before hydrolysis. The free-sugar and oligosaccharide profile of extracts and membrane streams was checked by high-performance liquid chromatography with a refractive-index detector. The inulin purity of the powder was expressed as the mass fraction of inulin in total dry solids. Moisture content was determined gravimetrically by oven drying to constant mass at 105 °C. Spray-drying yield was calculated as the mass of solids recovered as powder divided by the mass of solids fed. Solubility was assessed by the time required to obtain a homogeneous dispersion in water at 25 °C. Powder morphology was examined by scanning electron microscopy, and the physical state (amorphous versus crystalline) was checked by X-ray diffraction. Indicative microbial cleanliness was evaluated by standard aerobic plate counts. Protein content was estimated colourimetrically to track removal across the membrane stages.

3. RESULTS AND DISCUSSION

3.1. Process Overview

Figure 2 shows the integrated workflow as operated in this study. The three blocks — extraction, membrane purification, and drying — are connected so that the output of one stage is the feed of the next, and the nanofiltration permeate is shown as a recoverable side stream rather than waste. The following sections report the optimisation and the observed performance of each block, together with the practical difficulties encountered. In full, the train comprises root pre-treatment (vibro screening and hammer milling), hot-water extraction, coarse drum and 25 µm press filtration, lime/acid clarification with decanting and activated-carbon/Hyflo treatment, microfiltration, nanofiltration with diafiltration and concentration from about 7 °Brix to 15 °Brix, demineralisation on anion and cation ion-exchange resin columns, multiple-effect evaporation from about 15 °Brix to 35 °Brix, and spray drying, followed by packing and storage. Spent root solids separated during filtration are recovered as a by-product stream — dewatered in a screw press, sun-dried, and used as boiler feed — alongside the nanofiltration permeate, which remains a recoverable source of fructooligosaccharides.

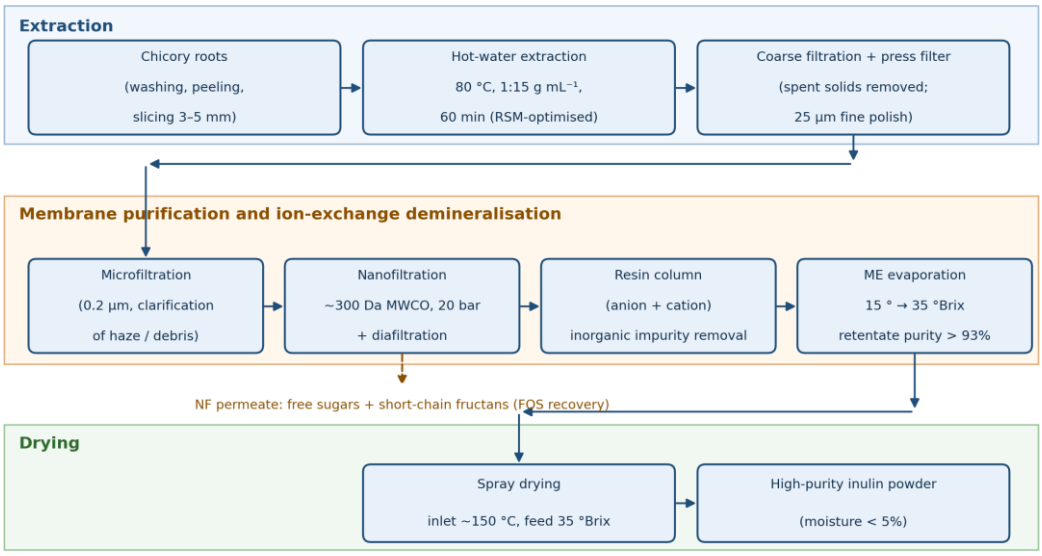

Figure 2. Integrated membrane-assisted process for producing high-purity inulin powder from chicory roots, showing coarse filtration with a 25 µm press filter, followed by microfiltration, nanofiltration with diafiltration, anion–cation ion-exchange demineralisation, multiple-effect evaporation, and spray drying. The nanofiltration permeate, enriched in free sugars and short-chain fructans, is treated as a recoverable side stream for potential fructooligosaccharide recovery.

3.2. Optimisation of Hot-Water Extraction

The Box-Behnken design results indicated that all three factors affected the recovery of inulin to varying magnitudes. The quadratic model has a significant lack-of-fit ($p = 0.18$), which was not significant ($p < 0.001$), with R^2 and adjusted R^2 values of 0.972 and 0.936, respectively, indicating that the model was satisfactory for describing the responses. The temperature (X_1) was the most significant and high coefficient of the linear terms ($p < 0.001$); solid liquor ratio (X_2) was significant term ($p < 0.01$), but weaker term than (X_1); the term time (X_3) was significant in the second position ($p < 0.05$), acting as a weaker term compared to (X_2 and X_1). The negative quadratic term for temperature (X_1^2; $p < 0.01$) showed that the response was curved and that there was an interior optimum, i.e., nonlinear instead of monotonically increasing. The only significant interaction found was the temperature–time interaction (X_1X_3), but this agrees with both factors playing a role in overall thermal exposure.

The result of the effects of temperature is shown in Fig. 3(a) with error bars from 3 times runs. As the solvent viscosity was decreased, more inulin was recovered from the tissue, with the percentage of recovery going up rapidly from 58.4 ± 2.1% at 60 °C to 84.2 ± 1.5% at 80 °C due to greater diffusion. Only between 80 and 90 °C, a slight gain (85.6 ± 1.9%) could be noticed, which caused a decrease of the molecular weight fraction of high molecular weight from 81% to 73%, suggesting that the additional heat mainly resulted in partial hydrolysis and pigment release, not in useful recovery. The practical reasons for this trade-off are actually that the optimum was not set to the "highest" temp. Recovery increased with more dilute proportions of solid-to-liquid and with time due to the importance of sustaining a "steeper concentration gradient," and due to having "approached equilibrium" with time.

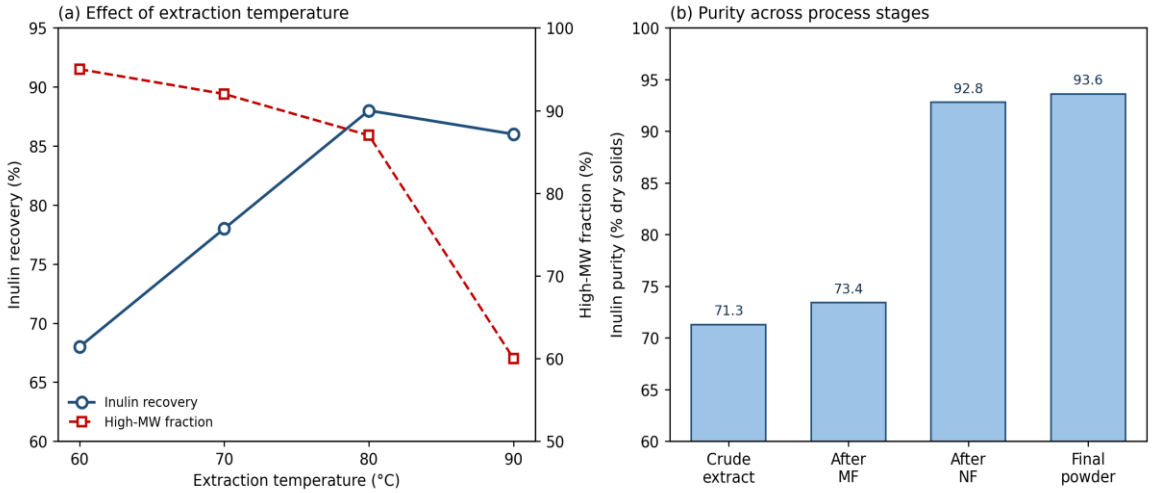

Figure 3. (a) Inulin recovery and the retained high-molecular-weight fraction at various extraction temperatures (shaded area is optimum). (b) Purity of inulin at different stages in the process. Error bars are the standard deviation of the triplicate measurements.

A maximum of 80 °C, 60 min, and 1:15 g mL-1 of solid-to-liquid ratio were obtained through numerical optimisation of the model: the maximum recovery was 84.2 ± 1.5 % (about 3 % close to the theoretical value of 86.7 %), which supports the model. The recovery falls within the range of those found for the optimised hot-water extraction of inulin from chicory reported by [4] and [6]. It should be noted that this is an optimum compromise: Running hotter and longer would increase the recovery by only a few per cent, but there would be a definite decrease in product quality, so the balance is in favour of product quality as opposed to the marginal benefit from running a little hotter. The design variables, along with the optimised condition, are put in Table 1.

Table 1. Box-Behnken design variables, coded levels, and the optimised hot-water extraction condition.

Factor	−1	0	+1	Optimum	Significance
X_1: Temperature (°C)	60	75	90	80	$p < 0.001$
X_2: Solid-to-liquid (g mL^{-1})	1:10	1:15	1:20	1:15	$p < 0.01$
X_3: Time (min)	30	60	90	60	$p < 0.05$
Response: recovery (%)	—	—	—	84.2 ± 1.5	$R^2 = 0.972$

The complete design matrix, with the coded factor levels and the inulin recovery measured for each of the 17 runs, is given in Table 2. The five centre-point runs (runs 13–17) gave closely grouped recoveries between 76.8 and 78.9%, which indicates good repeatability and provides the pure-error estimate used in the lack-of-fit test.

Table 2. Box-Behnken design matrix in coded factor levels and the measured inulin recovery for each run.

Run	X_1 (temp.)	X_2 (S:L ratio)	X_3 (time)	Recovery (%)
1	−1	−1	0	62.1
2	+1	−1	0	79.4
3	−1	+1	0	68.7
4	+1	+1	0	82.6
5	−1	0	−1	60.5
6	+1	0	−1	78.2
7	−1	0	+1	66.9
8	+1	0	+1	81.0
9	0	−1	−1	70.3
10	0	+1	−1	74.1
11	0	−1	+1	73.8
12	0	+1	+1	79.5
13	0	0	0	77.6
14	0	0	0	78.2
15	0	0	0	78.9
16	0	0	0	76.8
17	0	0	0	78.0

Coded levels: X_1 temperature (−1 = 60 °C, 0 = 75 °C, +1 = 90 °C); X_2 solid-to-liquid ratio (−1 = 1:10, 0 = 1:15, +1 = 1:20 g mL^{-1}); X_3 time (−1 = 30 min, 0 = 60 min, +1 = 90 min). Recovery values are means of triplicate measurements (pooled SD ≈ 1.8%).

A practical difficulty during extraction was the variability of the raw material. Even within one lot, root chips differed in inulin content by roughly ±4% relative, which is part of the scatter visible in the error bars. Feedstock variability of this kind is familiar in inulin processing, and it implies that lot-to-lot standardisation would be needed before any scale-up.

3.3. Membrane Purification and Fouling Behaviour

The inulin purity of the crude extract obtained at the optimum condition was only 71.3 ± 2.4% of dry solids due to the presence of short-chain oligosaccharides, free fructose and glucose, soluble proteins, and coloured phenolics. The function of microfiltration was primarily to clarify the water, removing haze and small particles, with purification slightly improved to 73.4 ± 2.2%, which was due to the fact that most of the impurities were in the dissolved state. The decisive gain in purity came with the implementation of nanofiltration. High-molecular-weight inulin was retained in the membrane, and the majority of the low molecular weight solutes were transferred to the permeate, leading to an 10%

increase in inulin purity in the retentate after diafiltration to 93.6 ± 1.3%. High-molecular-weight inulin was retained in the membrane, and the level of low molecular weight solute permeated into the permeate, showing an obvious decrease in colour after diafiltration. The inulin purity of the retentate improved to 93.6 ± 1.3%. This is illustrated in Figure 3(b). HPLC analysis of the permeate showed that it contained an increased amount of free sugars and short-chain oligosaccharides; as such, it is not regarded here as waste, but it is possible to recover the fructooligosaccharides.

But working with the membrane was not without its problems. The permeate flux of the nanofiltration stage decreased by approximately 30–35% throughout each run from approximately 42 to 28 Li?-2h-1, which was attributed to protein adsorption and formation of a partially gelled inulin layer at the membrane surface (concentration polarisation and fouling). Some flux was recovered during water flushing between runs, but a complete alkaline clean had to be performed to regain baseline specifications, and the diafiltration step also used a large amount of water and processing time to achieve high purity parameters. These observations are in line with the expected general behaviour during the membrane purification of inulin extracts [5, 9] and are the major operating parameters of the purification process. To achieve a realistic scale-up, the cleaning cycles, membrane life, and the cost of diafiltration water should be considered. The two membrane stages also resulted in measurable losses of inulin in the permeate, about 8–10% of the inulin fed to the membrane section, which is the main yield loss of the purification-based approach. Table 3 gives the levels of purity up to which the nulDATA is available and the associated streams.

Table 3. Inulin purity, protein removal, and stream observations across the integrated process.

Process stream	Inulin purity (%)	Protein removed (%)	Observations
Crude hot-water extract	71.3 ± 2.4	—	Turbid, coloured; free sugars and proteins present
After microfiltration	73.4 ± 2.2	≈ 12	Clear permeate; haze and debris removed
After nanofiltration + diafiltration	93.6 ± 1.3	≈ 78	Flux decline 30–35%; colour markedly reduced
Final spray-dried powder	92.8 ± 1.5	≈ 78	Small purity change within measurement scatter

3.4. Ion-Exchange Demineralisation and Concentration

Passing the nanofiltration concentrate over the two-bed resin column removed the residual inorganic load that the membrane stages could not, and the effect was followed as a fall in the conductivity of the liquor across the beds together with a visible lightening of colour, the weakly basic anion resin also retaining part of the remaining organic acids and colour bodies. Because ion exchange removes ash rather than organic impurity, its contribution to the purity figures in Table 3 is small: the purity of the demineralised stream remained within the measurement scatter of the value recorded after nanofiltration and diafiltration. The practical value of the step therefore lies in the ash content and conductivity of the final powder rather than in the purity number itself, which matters for a material intended for pharmaceutical use.

The cost of the step is operational rather than analytical. Bed capacity fell as each cycle progressed, and regeneration was required between batches; this consumes acid, alkali and rinse water and produces a saline effluent, and it also introduces additional hold-up and dilution through the rinse volumes. At laboratory scale these penalties are easily absorbed, but at larger scale they would have to be counted against the benefit of demineralisation. Multiple-effect evaporation of the demineralised liquor from about 15 °Brix to about 35 °Brix proceeded without incident under vacuum; no browning was observed and no measurable change in inulin purity was detected across the evaporator, which is consistent with the low boiling temperature used.

3.5. Spray Drying and Powder Properties

The inlet air temperatures and the feed solids had an influence on the dried product. The powder had high residual moisture (about 7 – 8%) and tended to cake, when the inlet was raised to 150 °C for the moisture reduction is to 4.6 ± 0.3% and Flow improvement is noted rather than any further moisture reduction was realized, and also the inlet temperature was raised to 170 °C, moisture was slightly reduced and it was noted that there was increase in thermal loading for a heat sensitive carbohydrate. Particles and solids throughput were both influenced by the concentration of the feed, with a 16% solids concentration causing a high viscosity in the feed and resulting in high wall deposition, while a concentration of 8% solids produced fine particles and low solids throughput. A compromise performance was found with the intermediate feed (~12% solids). At an inlet temperature of 150 °C and 12% feed solids, the powder with the best performance was a free-flowing product with 4.6 ± 0.3% moisture, obtained at a yield of 68.9 ± 2.7%.

Modest yield, self-evident reason while operating. The well-established problem in the spray drying of sugar-rich materials, namely the deposition of a sticky film on the wall of the drying chamber, was observed. Most of the estimated 30% loss was due to this wall deposition, and not fines being lost in the cyclone. In a small laboratory dryer, the wall-to-volume ratio is unfavourable, so this loss would be expected to be lower on a larger scale, but this is a real limitation of the present main line of the process and a clear limitation for optimisation in the future, such as by varying the drying outlet temperature or co-drying with a small proportion of a higher glass transition temperature carrier. The optimisation and properties of the powders produced by spray-drying are summarised in Table 4.

The dried powder has been further analysed and the findings are presented in Figure 4. Figure 4(a) illustrates a single broad halo in the diffraction pattern that is characteristic of an amorphous solid. This result is summarised directly and is the report's physical form for spray-dried inulin [25] and further supports the description of this powder as being predominantly amorphous. The particle size distribution shown in Figure 4(b) is unimodal and right-skewed with a median diameter (D_{50}) of ~ 11 µm and most of the particles ranging between 0.05 and 0.02 m. The particle size distribution in this range is typical for solution-based two-fluid nozzle spray drying. Test for solubility revealed rapid and complete dissolution in water at 25 °C, which was due to the fine size of the particles and the amorphous property.

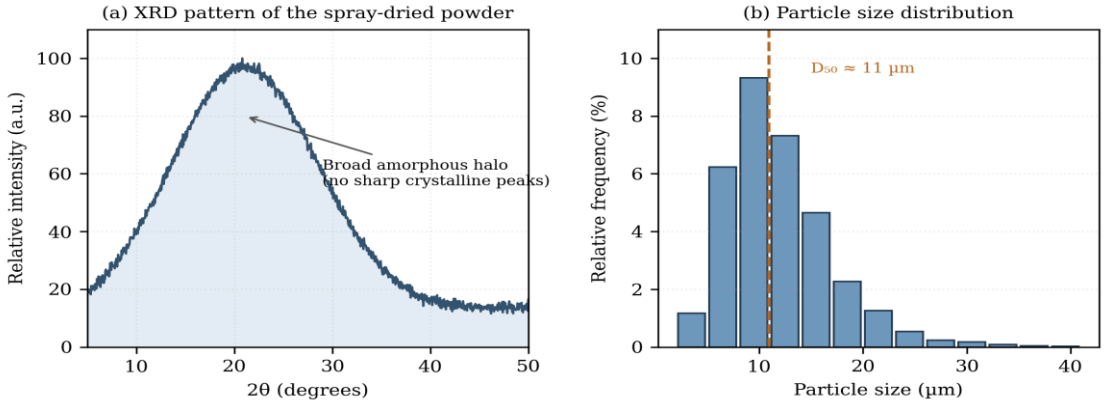

Figure 4. Characterisation of the spray-dried inulin powder. (a) X-ray diffraction pattern showing a broad amorphous halo with no crystalline peaks. (b) Particle size distribution, with the median diameter (D_{50}) marked.

Table 4. Effect of spray-drying conditions on powder properties, and the optimised result (feed solids fixed at 12% w/w for the temperature series).

Inlet temp. (°C)	Moisture (%)	Yield (%)	Observation
130	7.6 ± 0.5	61.2 ± 3.1	Cohesive, prone to caking
150 (optimum)	4.6 ± 0.3	68.9 ± 2.7	Free-flowing; moderate wall deposit
170	4.1 ± 0.4	66.4 ± 3.0	Higher thermal load; little extra benefit

3.6. Powder Quality and Benchmarking

The result is a powder with the characteristics that are usually required of a high-purity, pharmaceutical material productively manufactured by the integrated process. Its inulin purity of approximately 93% is well in excess of the usual contours concerning food grade inulins, which is usually worried about because reducing sugars, proteins and pigments, which are most commonly the contaminants of concern, are removed by nanofiltration. With a residual moisture lower than 90–92% and purity above 95%, the present powder is similar in purity, residual moisture, and — though the particle size D_{50} is approximately 11 µm — stability and endotoxin measurements would still have to be done, but were beyond the scope of the present invention. The remaining moisture content below 5% provides good physical stability and caking resistance, and the indicative aerobic plate counts of the final powder were low, reflecting both the cleanliness of the feed material used as an input into the dryer and the heat environment of the process. The form of the product is amorphous and free-flowing, and it is quickly absorbed. This corresponds with the properties of inulin as a carrier and protectant as described in Section 1. This retention of the highest molecular weight inulin is protected by the extraction optimum and the nanofiltration cut-off - it is therefore not a consequence of monomodal behaviour but is a feature of the product.

3.7. Process Integration, Trade-offs, and Limitations

Paralleling each of the three stages was the level of reliance they had on each other. While the recovery rate is decreased by about a few per cent with moderate extraction temperature, it simultaneously retains the high molecular weight inulin and permits less pigment to pass through, making the membranes' task easier and a lighter-colored powder is obtained. The 'cleaner' the small sugars, the less sticky it will be, and a feed that had both the small sugars removed by nanofiltration would be in a better place to pass on to the dryer than a crude extract would be [29]. This decision was made early, hence it is evident two levels later, hence why the workflow was thought through as a whole and not "one step at a time" etc.

It doesn't cost anything. The higher the extraction temperature, the higher the recovery, but the lower the polymer quality; the more diafiltration runs, the higher the purity, but the more water and time; if the extraction temperature is higher, it will be faster in the dryer, which will increase the thermal and energy cost. The operating point discussed in this paper could be one of several points that may be more economical for the particular processing situation.

Several restrictions need to be clearly outlined. The first is that all tests were conducted at laboratory scale, and fouling and wall deposition will not occur in the same manner at a larger scale and have not been tested in a pilot rig. Second, the total inulin yield is diminished by the loss of 8–10% of material into the membrane permeate and the loss of material

due to deposition in the dryer, compromising the yield for the purity. Third, the experimental scatter, plus the raw-material variability, would need to be controlled before scale-up (at approximately +/-4%). Fourth, purity, moisture content, state of aggregation, particle size, solubility, and indicative microbial testing were performed with the possibility that additional quality testing, such as molecular-weight distribution, endotoxins, stability testing and excipient qualification, could be conducted for pharmaceutical use. These are the limits of the present results.

4. CONCLUSION AND FUTURE WORK

In this study, an integrated process for high-purity inulin powder production by chicory roots, focused on the membrane-assisted process, was developed. The Box-Behnken optimisation identified an extraction condition of 84.2 ± 1.5% recovery with a modifiable molecular weight of large molecules without damage at a moderate extraction condition (80 °C, 1:15 g mL^{-1}, 60 min) that was sufficiently supported by a satisfactory explained variance ($R^2 = 0.972$), demonstrated by the model's statistical appropriateness. A microfiltration–nanofiltration sequence, followed by demineralisation on anion and cation ion-exchange resin columns and multiple-effect evaporation, improved the purity of inulin from 71.3% to 93.6% dry solids, and optimising spray drying conditions yielded a free-flowing amorphous powder containing 4.6% moisture with a yield of close to 69%. These results illustrate that the process of extraction, purification, and drying can be achieved as a single unit operation to show good inulin purity from a low-cost feedstock, as well as actual operational costs such as membrane fouling and drying losses.

Validation on a pilot scale of the membrane and drying step, molecular-weight distribution and stability of the powder, recovery of fructooligosaccharides from the nanofiltration permeate, and powder evaluation in representative delivery systems could be a part of future work. If there were any claim to be made to suitability for the pharmacopoeia, this type of study would need to be conducted before that could be done.

Conflict of Interest

The authors declare that there is no conflict of interest regarding the publication of this paper.

REFERENCES

1. Mensink, M.A., Frijlink, H.W., van der Voort Maarschalk, K. & Hinrichs, W.L.J. “Inulin, a flexible oligosaccharide I: Review of its physicochemical characteristics,” Carbohydrate Polymers, vol. 130, pp. 405–419, 2015. https://doi.org/10.1016/j.carbpol.2015.05.026
2. Shoaib, M., Shehzad, A., Omar, M., Rakha, A., Raza, H., Sharif, H. R., Shakeel, A., Ansari, A., & Niazi, S. (2016). Inulin: Properties, health benefits and food applications. Carbohydrate polymers, 147, 444–454. https://doi.org/10.1016/j.carbpol.2016.04.020
3. Apolinário, A. C., de Lima Damasceno, B. P., de Macêdo Beltrão, N. E., Pessoa, A., Converti, A., & da Silva, J. A. (2014). Inulin-type fructans: a review on different aspects of biochemical and pharmaceutical technology. Carbohydrate polymers, 101, 368–378. https://doi.org/10.1016/j.carbpol.2013.09.081
4. D. R. Manimaran, E. Swetha, S. Iswaryalakshmi, S. Sivamani; Optimization of inulin extraction from roots of Cichorium intybus. AIP Conf. Proc. 29 November 2022; 2446 (1): 020015. https://doi.org/10.1063/5.0108839
5. Sağcan, N., Sağcan, H., Bozkurt, F., Bulut Güneş, A. N., Fakir, H., Dertli, E., & Sağdıç, O. (2024). Optimization of Inulin Extraction from Chicory Roots and an Ultrafiltration Application to Obtain Purified Inulin and Hydrolyzed Fructooligosaccharides. Journal of Agricultural Sciences, 30(1), 166-178. https://doi.org/10.15832/ankutbd.1338572
6. Singh, M., Rani, H., & Chopra, H. K. (2025). Extraction, optimization, purification and characterization of inulin from chicory roots using conventional and greener extraction techniques. International journal of biological macromolecules, 306(Pt 1), 141385. https://doi.org/10.1016/j.ijbiomac.2025.141385
7. Hussain, S., Randhawa, M.A., Rakha, A. et al. Ultrasound-assisted extraction, quantification and characterization of inulin from agave, chicory and Jerusalem artichoke. Sci Rep 16, 11713 (2026). https://doi.org/10.1038/s41598-026-43085-8
8. Elnaz Milani, Arash Koocheki, Q Ali Golimovahhed, Extraction of inulin from Burdock root (Arctium lappa) using high intensity ultrasound, International Journal of Food Science and Technology, Volume 46, Issue 8, August 2011, Pages 1699–1704, https://doi.org/10.1111/j.1365-2621.2011.02673.x
9. Demirci, K., Zungur-Bastıoğlu, A., Görgüç, A., Bayraktar, B., Yılmaz, S. & Yılmaz, F.M. “Microwave irradiation, evolutionary algorithm and ultrafiltration can be exploited in process intensification for high-purity and advanced inulin powder production,” Chemical Engineering and Processing - Process Intensification, vol. 194, art. 109565, 2023. https://doi.org/10.1016/j.cep.2023.109565
10. Wei, L., Wang, J., Zheng, X., Teng, D., Yang, Y., Cai, C., Feng, T. & Zhang, F. “Studies on the extracting technical conditions of inulin from Jerusalem artichoke tubers,” Journal of Food Engineering, vol. 79, no. 3, pp. 1087–1093, 2007. https://doi.org/10.1016/j.jfoodeng.2006.03.028
11. Zhang X, Zhu X, Shi X, Hou Y, Yi Y. Extraction and Purification of Inulin from Jerusalem Artichoke with Response Surface Method and Ion Exchange Resins. ACS Omega. 2022 Mar 28;7(14):12048-12055. doi: 10.1021/acsomega.2c00302. PMID: 35449954; PMCID: PMC9016842
12. Termrittikul, P., Jittanit, W., & Sirisansaneeyakul, S. (2018). The application of ohmic heating for inulin extraction from the wet-milled and dry-milled powders of Jerusalem artichoke (Helianthus tuberosus L.) tuber. Innovative Food Science & Emerging Technologies, 48, 99–110. https://doi.org/10.1016/j.ifset.2018.05.022
13. Khuenpet, K., Fukuoka, M., Jittanit, W., & Sirisansaneeyakul, S. (2017). Spray drying of inulin component extracted from Jerusalem artichoke tuber powder using conventional and ohmic-ultrasonic heating for extraction process. Journal of Food Engineering, 194, 67–78. https://doi.org/10.1016/j.jfoodeng.2016.09.009

14. Junyusen, P., Taengsopha, P., Labut, K., Chatchavanthatri, N., & Junyusen, T. (2026). Process development for producing high-purity inulin powder from Jerusalem artichokes through hot water extraction, purification, and drying. LWT, 245, 119267. https://doi.org/10.1016/j.lwt.2026.119267
15. Petkova, N., Hambarliyska, I., Ivanov, I., Ognyanov, M., Nikolova, K., Ibryamova, S., & Ignatova-Ivanova, T. (2025). Physicochemical, Functional, and Antibacterial Properties of Inulin-Type Fructans Isolated from Dandelion (Taraxacum officinale) Roots by "Green" Extraction Techniques. Applied Sciences, 15(8), 4091. https://doi.org/10.3390/app15084091
16. Alexsandra Conceição Apolinário, Martins, E., Ponciano, B., Silva, Attilio Converti, Pessoa, A., & Gonzalez, A. (2017). Extraction, isolation and characterization of inulin from Agave sisalana boles. 108, 355–362. https://doi.org/10.1016/j.indcrop.2017.06.045
17. Redondo-Cuenca, A., Herrera-Vázquez, S. E., Condezo-Hoyos, L., Gómez-Ordóñez, E., & Rupérez, P. (2021). Inulin extraction from common inulin-containing plant sources. Industrial Crops and Products, 170, 113726. https://doi.org/10.1016/j.indcrop.2021.113726
18. Lopes, S. M. S., Krausová, G., Carneiro, J. W. P., Gonçalves, J. E., Gonçalves, R. A. C., & de Oliveira, A. J. B. (2017). A new natural source for obtainment of inulin and fructo-oligosaccharides from industrial waste of Stevia rebaudiana Bertoni. Food Chemistry, 225, 154–161. https://doi.org/10.1016/j.foodchem.2016.12.100
19. Stökle, K., Jung, D., & Kruse, A. (2020). Acid-assisted extraction and hydrolysis of inulin from chicory roots to obtain fructose-enriched extracts. Biomass Conversion and Biorefinery. https://doi.org/10.1007/s13399-020-01108-y
20. Zhu, Z., Bals, O., Grimi, N., & Vorobiev, E. (2012). Pilot scale inulin extraction from chicory roots assisted by pulsed electric fields. International Journal of Food Science & Technology, 47(7), 1361–1368. https://doi.org/10.1111/j.1365-2621.2012.02981.x
21. Zhang, R., Vorobiev, E., Zhu, Z., & Grimi, N. (2021). Effect of pulsed electric fields pretreatment on juice expression and quality of chicory. Innovative Food Science & Emerging Technologies, 74, 102842. https://doi.org/10.1016/j.ifset.2021.102842
22. Rivera, A., Pozo, M., Sánchez-Moreno, V. E., Vera, E., & Jaramillo, L. I. (2024). Pulsed Electric Field-Assisted Extraction of Inulin from Ecuadorian Cabuya (Agave americana). Molecules, 29(14), 3428. https://doi.org/10.3390/molecules29143428
23. Ram Sarup Singh, Rupinder Pal Singh, & Kennedy, J. F. (2016). Recent insights in enzymatic synthesis of fructooligosaccharides from inulin. International Journal of Biological Macromolecules, 85, 565–572. https://doi.org/10.1016/j.ijbiomac.2016.01.026
24. Wang, Z., Ling, N., Guo, C., Tian, H., Gao, M., Li, W., & Ji, C. (2025). Deciphering inulin from Jerusalem artichoke: Extraction, structural characteristics, bioactivities, structure-activity relationship, modifications, pharmacokinetics and applications. Phytomedicine, 147, 157219. https://doi.org/10.1016/j.phymed.2025.157219
25. M.Z. Saavedra-Leos, C. Leyva-Porras, E. Martínez-Guerra, S.A. Pérez-García, J.A. Aguilar-Martínez, & C. Álvarez-Salas. (2014). Physical properties of inulin and inulin–orange juice: Physical characterization and technological application. Carbohydrate Polymers, 105, 10–19. https://doi.org/10.1016/j.carbpol.2013.12.079
26. Araujo-Díaz, S. B., Leyva-Porras, C., Aguirre-Bañuelos, P., Álvarez-Salas, C., & Saavedra-Leos, Z. (2017). Evaluation of the physical properties and conservation of the antioxidants content, employing inulin and maltodextrin in the spray drying of blueberry juice. Carbohydrate Polymers, 167, 317–325. https://doi.org/10.1016/j.carbpol.2017.03.065
27. Toneli, J., Park, K., Negreiros, A., & Murr, F. (2010). Spray-Drying Process Optimization of Chicory Root Inulin. Drying Technology, 28(3), 369–379. https://doi.org/10.1080/07373931003645017
28. Beirão-da-Costa, S., Duarte, C., Bourbon, A. I., Pinheiro, A. C., Januário, M. I. N., Vicente, A. A., Beirão-da-Costa, M. L., & Delgadillo, I. (2013). Inulin potential for encapsulation and controlled delivery of Oregano essential oil. Food Hydrocolloids, 33(2), 199–206. https://doi.org/10.1016/j.foodhyd.2013.03.009
29. Sobulska, M., & Zbicinski, I. (2020). Advances in spray drying of sugar-rich products. Drying Technology, 1–26. https://doi.org/10.1080/07373937.2020.1832513
30. Graciele Lorenzoni Nunes, Mariana, Alexandre José Cichoski, Leila Queiroz Zepka, Eduardo Jacob Lopes, Emanuelli, T., Erico M.M. Flores, Silva, & Cristiano. (2018). Inulin, hi-maize, and trehalose as thermal protectants for increasing viability of Lactobacillus acidophilus encapsulated by spray drying. 89, 128–133. https://doi.org/10.1016/j.lwt.2017.10.032
31. Arslan-Tontul, S., & Erbas, M. (2017). Single and double layered microencapsulation of probiotics by spray drying and spray chilling. LWT - Food Science and Technology, 81, 160–169. https://doi.org/10.1016/j.lwt.2017.03.060
32. Bustamante, M., Oomah, B. D., Rubilar, M., & Shene, C. (2017). Effective Lactobacillus plantarum and Bifidobacterium infantis encapsulation with chia seed (Salvia hispanica L.) and flaxseed (Linum usitatissimum L.) mucilage and soluble protein by spray drying. Food Chemistry, 216, 97–105. https://doi.org/10.1016/j.foodchem.2016.08.019
33. Fritzen-Freire, C. B., Prudêncio, E. S., Amboni, R. D. M. C., Pinto, S. S., Negrão-Murakami, A. N., & Murakami, F. S. (2012). Microencapsulation of bifidobacteria by spray drying in the presence of prebiotics. Food Research International, 45(1), 306–312. https://doi.org/10.1016/j.foodres.2011.09.020
34. Kuhn, F., Azevedo, E. S., & Pelayo, C. (2020). Behavior of inulin, polydextrose, and egg albumin as carriers ofBougainvillea glabrabracts extract: Rheological performance and powder characterization. Journal of Food Processing and Preservation, 44(10). https://doi.org/10.1111/jfpp.14834